



13th COTA International Conference of Transportation Professionals (CICTP 2013)

## Multi-fractal Analysis for Pavement Roughness Evaluation

Wei Quan<sup>a</sup>, Hua Wang<sup>a\*</sup>, Xin Liu<sup>a</sup>, Shen Zhang<sup>a</sup><sup>a</sup>*Harbin Institute of Technology. No.73, Huanghe Road, Nangang District, Harbin, 150090, China*

---

### Abstract

The paper employs multi-fractal theory to systematically research into appraising the road profile in order to overcome the shortages of the current used road roughness indices which cannot fine depict the characteristics of the road locally. The paper proves the road profile has the obvious multi-fractal characteristics. On this basis, multi-fractal spectrum and the parameters can be used in the research of the road profile. The results of road surface simulation results in each grades based on Fourier inverse transformation show there is no unique relation between multi-fractal spectral width and road roughness in different grades, while the vertical axis, intercept of the roads that have the same multi-fractal spectral width was different in Logarithmic distribution of measure and scale. Finally, the combination of multi-fractal spectral width and the IRI is proposed as supplement of current indices when necessary.

© 2013 The Authors. Published by Elsevier Ltd. Open access under [CC BY-NC-ND license](#).

Selection and peer-review under responsibility of Chinese Overseas Transportation Association (COTA).

*Keywords:* road roughness; multi-fractal theory; body bump index; IRI;

---

### 1. Introduction

There are many measurement methods and apparatus for achieving road roughness, as well as many varied evaluation indexes correspondingly. The road roughness indices currently used cannot fine depict the characteristics of the road locally, which are summarized as follows: (1) International Roughness Index (IRI). IRI can describe the amplitude of road roughness and the wavelength change of the natural frequency to some extent, but not sensitive to the road surface waves in other frequency range; furthermore, 1/4 vehicle models involved in the calculation can't reflect the influence upon human comfort which arises from the vehicle pitch vibration, the lateral swing as well as the front and rear wheels. (2) Ruler to measure the maximum gap value. Low detection efficiency, workload, and accuracy do not meet the present requirements, which cannot measure the long-wavelength pavement, and human factors exert greater impact on the measurement results. (3) The roughness standard deviation ( $\sigma$ ). By using computer to simulate the roughness standard deviation, it is found that a

---

\* Corresponding author. Tel.: +86-451-86283036.

E-mail address: [wanghua@hit.edu.cn](mailto:wanghua@hit.edu.cn)

completely different road might have the same  $\sigma$ ; therefore, its value cannot truly reflect the road traveling comfort is good or bad. (4) The power spectral density (PSD). The PSD can demonstrate the information of the pavement wavelength or frequency distribution and summarize the general characteristics of the road, but as other indicators, it still cannot well reflect the vehicle and human factor. (5) Plane index (PI). During the measurement, the perception of the mapping wheel on the comparable flat road surface may be less keen, it is also not suitable to measure roads with more pits or damages, the traveling speed in the measurement process may be not too fast. (6) The RMS of the vertical acceleration (RMSVA). RMSVA, classified in the PQI index, reflects the ride quality. It can be conversed with IRI through the calibration tests, but not fully reflecting the road conditions is its shortcoming.

A new analysis and evaluation technology is preferred to extract the concrete information of the pavement longitudinal profile or the complement of the existing evaluation to perfect the pavement roughness evaluation methods. Observed from the whole road surface, it is easily to find the road is undulating, and does not follow a certain variation; but if observed locally, the greater fluctuation is combined with many smaller undulations, while the smaller ups and downs of roads are similar with the overall surface. When analyzing the fractal characteristics of road roughness by using the method of power spectral, it is found the scale-free interval can be approximated in two straight lines in the double logarithmic plot that means there are two scale-free intervals [8]. If observing the two scale-free intervals, we can find that each fractal behavior has its own upper and lower limit, while the single fractal theory only conduct research and analysis on one interval. Therefore, it is preferable to apply the multi-fractal analysis technology to the study of the road roughness, and propose the multiple fractal dimension spectrum analysis and evaluation methods of the road roughness to obtain the deep level research results of the road roughness.

## 2. MF-DFA Research Method based on the Sliding Windows

### 2.1. The MF-DFA Based on the Sliding Windows

The specific procedures of this method are as follows:

1) Calculate the cumulative deviation  $\{y_i\}$  of the sequence to the mean value; merge the original sequence into a new sequence by summing:

$$y_i = \sum_{k=1}^i x_k - \bar{x}, \quad i = 1, 2, \dots \quad (1)$$

2) Split the sequence  $\{y_i\}$  into equal long small pieces. Divide the sequence  $\{y_i\}$  into the overlapping subparagraph (N-S+1) with the sliding window length  $s$ ; on each short  $v$ , obtained the local trend function of the segment by using the least squares method, referred to as  $P_v(j)$ , it can be the polynomial fitted by linear, quadratic or higher order form. Then eliminate the trend of each segment, its residual sequence is as follows:

$$Z_{vj} = Y(j) - P_v(j) \quad (2)$$

3) Calculate the square mean value of the (N-S+1) sub-intervals which eliminate the trend sequence, i.e. for the length of each split  $S$ , we can obtain the corresponding wave function value  $F_q(s)$ , it can be expressed as (3)

$$\begin{cases} F_q(s) = \left\{ \frac{1}{N-S+1} \sum_{v=1}^{N-S+1} [F^2(s, v)]^{\frac{q}{2}} \right\}^{\frac{1}{q}}, & q \neq 0 \\ F_q(s) = \exp \left\{ \frac{1}{2(N-S+1)} \sum_{v=1}^{N-S+1} \ln [F^2(s, v)] \right\}, & q = 0 \end{cases} \quad (3)$$

4) Taking different  $q$  values of (3) to obtain the corresponding  $F_q(s)$  value, then analyzing the relationship between  $F_q(s)$  and  $s$ , that is  $F_q(s) \propto s^{h(q)}$ . The function diagram of  $\ln[F_q(s)] \sim \ln(s)$  is achieved after taking the logarithm from the two sides of the relation, besides, we can find that the slope of the line is the  $q$ -order

generalized Hurst exponent  $h(q)$ . Additionally, introducing the fitting formula within the entire range of order  $q$  proposed by Koscielny-Bunde, as follows:

$$h(q) = \frac{1}{q} - \frac{\ln(a^q + b^q)}{q \ln 2} \quad (4)$$

5) The promotion of the order model can be calculated by (5) and the specific derivation process is in the references<sup>[11]</sup>.

$$\tau(q) = -\frac{\ln(a^q + b^q)}{\ln 2} \quad (5)$$

6) The multi-fractal odd spectrum  $f(a)$  can be calculated by (6).  $a$  means the odd degree of each sub-interval in the sequence;

$$\begin{cases} a = -\frac{1}{\ln 2} \frac{a^q \ln a + b^q \ln b}{a^q + b^q} \\ f(a) = -\frac{q}{\ln 2} \frac{a^q \ln a + b^q \ln b}{a^q + b^q} + \frac{\ln(a^q + b^q)}{\ln 2} \end{cases} \quad (6)$$

## 2.2. Influence from the value range of weighting factor

In the multi-fractal theory, the range of  $q$  is from negative infinity to positive infinity. However, in the actual calculation process, if the value of  $|q|$  increases continuously, then the level of analysis and the values needed to calculate such as the  $F_q(s)$  will increase exponentially, which invisibly increase the workload of the computer. When  $q$  reaches at a certain extent, the computer is bound to bring about overflow error and thus ends the entire calculation process; while if the initial range of  $q$  is too small, even if small changes occurring upon  $|q|$  can lead to larger changes of  $f(a)$ , which can't fully reflect the multi-fractal spectral nature of the sequence itself under such circumstance. In addition, when the value of  $q$  reaches a certain value, the increased value of  $q$  also had no significant effect upon the calculated results, which means the multi-fractal spectrum spectral width changes is small. It is urgent to formulate a standard to measure whether the range of  $q$  is reasonable.

Table 1 shows the results of spectral width values of selecting five road sections.

Table 1 the spectral width values of the different  $q$  value

section	$q$	$\Delta a$
1	20	0.53897
	23	0.53905
	25	0.53928
2	20	0.46132
	23	0.46208
	25	0.46312
3	20	0.40176
	23	0.40183
	25	0.40201
4	20	0.45103
	23	0.45116
	25	0.45122
5	20	0.60421
	23	0.60428
	25	0.60432

From Table 1, we can see that the spectrogram of the smaller  $q$  value is only a part of the larger one, but as for the 1st section, when  $q$  changes from 20 to 25, the change of  $\Delta a$  is only 0.00031, it can be considered the increased value of  $q$  spectrogram is very small, therefore, we can regard the less than 0.1%  $|\Delta a_{\max}|/\Delta a$  and  $|\Delta a_{\min}|$

$|\Delta a$  (that is, the rate change of  $\Delta a < 0.2\%$ ) as the  $q$  value standard, in which  $da_{\max}$  means the change of  $a_{\max}$   $|da_{\min}|/|\Delta a|$  when the value of  $q$  increases 1, and  $da_{\min}$  means that the change of  $a_{\min}$  when the value of  $q$  increases 1,  $\Delta a$  means the multi-fractal spectrum width. Only when the range of  $q$  meets this standard, it can be considered as the reflection of the sequence of the uneven distribution of the multi-fractal spectrum.

### 3. Time Power Spectral Density Representation

Road random excitation refers to the pavement roughness will exert some vibration during vehicle running; moreover, the car travel speed will affect the intensity of the vibration. The relationship between the time power spectral density of the road roughness  $G_q(f)$  in the time and frequency range of  $f_l < f < f_u$  and the space power spectral density of the road roughness can be expressed as follows<sup>[8][18]</sup>:

$$G_q(f) = \frac{1}{u} G_q(n) = \frac{1}{u} G_q(n_0) \left(\frac{n}{n_0}\right)^{-w} = G_q(n_0) n_0^w \frac{u^{w-1}}{f^w} \quad (7)$$

After giving the spatial power spectral density values and the discrete frequencies  $f_k$  ( $k=0, 1, \dots, N-1$ ) of the road section, each parameter of the (7) is assigned so that the time power spectral density  $G_q(f_k)$  of the road roughness at a given frequency will be easily calculated.

$$G_k(f_k) = \frac{2}{N\Delta t} \left| \sum_{n=0}^{N-1} x(n) e^{-j2\pi f_k n \Delta t} \right|^2 = \frac{2\Delta t}{N} |X_k|^2 = \frac{2}{\Delta f N^2} |X_k|^2 \quad (8)$$

Based on the (3), further figuring out the spectral amplitude  $|Q_k|$  corresponding to the  $G_q(f_k)$ :

$$Q(k) = |Q(k)| e^{j\phi_k} \quad (9)$$

where  $\phi_k$  refers to the frequency spectral phase.

For the discrete sampling points of the road random excitation, its frequency spectral amplitude has a close relation with its time power spectral density, that is, the time domain and frequency domain discrete points meet (8). Therefore, if conducting the Fourier inverse transform on the phase information of the road random excitation spectrum, you can get the time domain representation of the road random excitation.

To make the simulated road roughness be close to the reality as far as possible, we can't ignore the randomness of the road roughness. Specifically, the road random phase of the excitation spectrum is characterized by the randomness. By the existing literature, the phase  $\phi_k$  can be taken as the random variable equally distributed in the  $(0, 2\pi)$ . Since the amplitude and phase are already the known quantity, the time-domain representation  $q(n)$  of the road random excitation from the (9) and  $q(n)$  is a sequence of real numbers.

From (7) to (9), we can easily find that the simulation process is essentially the inverse process of computing the road surface power spectral density. Theoretically, as long as the sampling time interval meets the requirements of the sampling theorem, the simulated road roughness power spectral density and the initial calculating power spectral density are the exactly same, i.e. the two curves in the power spectral density map are completely coincident.

In the spatial frequency range of  $0.01 \sim 3 \text{ m}^{-1}$ ,  $\Delta l = 0.1 \text{ m}$ ,  $L = 819.2 \text{ m}$ , stimulating road roughness, so the sample pointing  $N = L/\Delta l = 8192$ , and the spatial frequency interval  $\Delta n = 1/L = 0.00122 \text{ m}^{-1}$ .

Referring to the spatial frequency, Fig. 1 is the pavement elevation graph which is generated from the simulated road roughness index  $G_d(n_0) = 8, 32$  under the condition of the frequency index  $w = 2$ . In Fig. 1, the abscissa is the longitudinal length along the road, and the ordinate is the height of the actual road surface relative to the reference plane. Fig. 2 is the comparison diagram between the initially given power spectral density and the power spectral density derived from the original data of the two levels road roughness. Fig. 2 shows the road roughness calculated from the given power spectral density after the Fourier inverse transform has guaranteed its power spectral density and the given power spectral density are exactly same, the analog value and the analytical value completely overlap, exactly the same as actual results and theoretical results, which illustrate the feasibility and correctness of the method to simulate the road roughness based on the inverse Fourier transform.

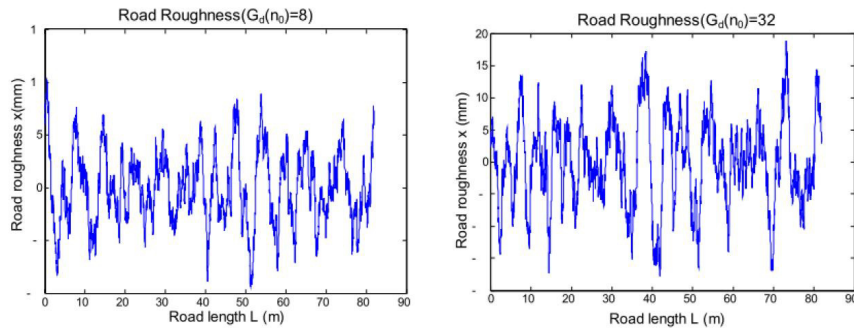


Fig.1. Simulated road roughness

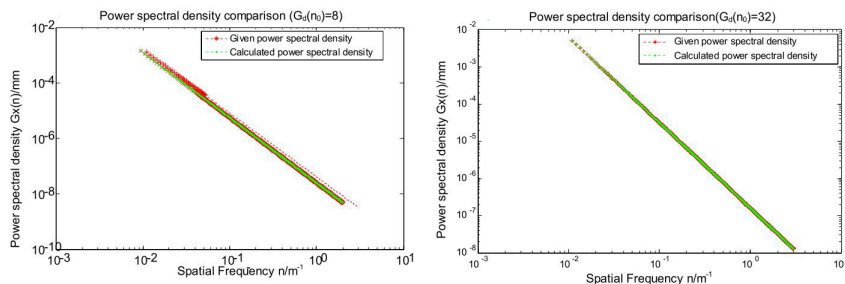


Fig.2 Relationship between power spectral density and the given power spectral density

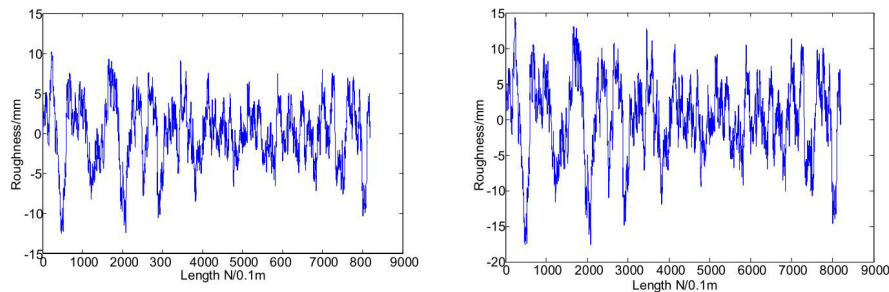


Fig.3. Road roughness of (a) The original pavement; (b) The pavement stretched 1.4214 times

#### 4. Relativity of Multi-fractal Spectrum Spectral Width Value

Fig. 3(b) is 1.4142 times the amplitude of the expansion of the original road roughness sequence, which is to stretch (a) in longitudinal direction, which still takes advantage of the multi-fractal method to determine the multi-fractal characteristics of the two curves, as shown in Fig.4.

The multi-fractal spectral width value has relativity shown in Fig.4. The multi-fractal spectrum of the original pavement and the pavement stretched 1.4214 times are same after the calculation based on the MF-DFA method of the sliding window: the maximum values of  $a$  are all 1.3417, the minimum values of  $a$  are 0.80685, and the spectral width values are 0.53483. Further verify that, no matter how many times the amplitude of the road roughness of Fig. 3(a) longitudinally stretched or shrunk, the calculated multi-fractal spectrum is still consistent with original data. By understanding of the multi-fractal principle, we can find that the multi-fractal spectrum is

related to the slope value of the straight measured by multi-scale, which means that under the condition of the slope unchanged, by moving the straight in the double logarithmic graph, the same multi-fractal spectrum graph can be achieved. This phenomenon shows that the multi-fractal spectral width value has nothing to do with the size of the absolute value; the calculation process is only a process of the relative parameters selected.

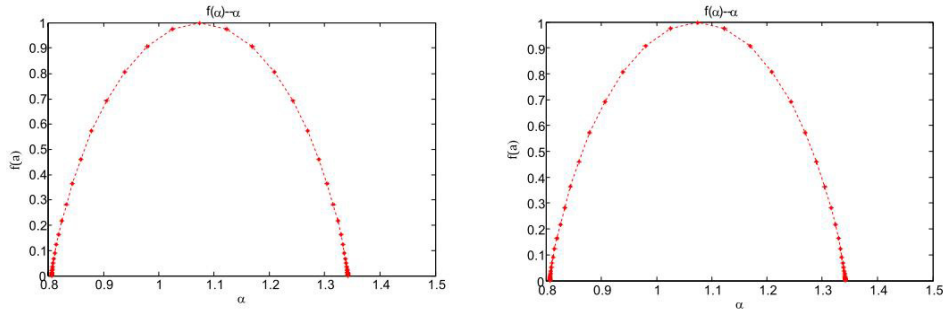


Fig.4. Multi-fractal spectrum. (a) The original pavement; (b) The pavement stretched 1.4214 times

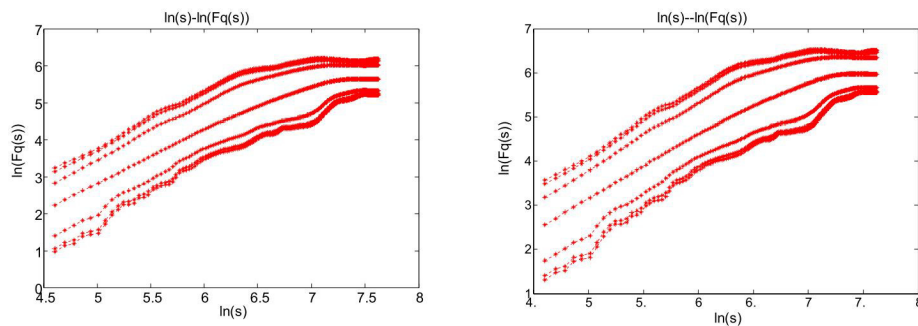


Fig. 5. Double logarithmic graph. (a) Original pavement; (b) Pavement stretched 1.4214 times ( $q = -50, -30, -10, 0, 10, 30, 50$  from top to bottom)

Fig. 5 shows the amplitude of the road roughness sequence's multi-fractal spectrum graph longitudinally stretched before and after are the same, but we can find from its double logarithmic graph: the intercept of the  $q = 0$  line on the vertical axis is different, the expanding multiples greater, i.e. the pavement more uneven, and the intercept greater. As shown in Fig. 5 (a), the intercept of the line  $q = 0$  is -2.2959, (b) is -1.9493, there are significant differences between the two. Therefore, the intercept of the  $q = 0$  line on the vertical axis in the double logarithmic graph can distinguish the measured absolute value of the road roughness.

Through the above analysis, the multi-fractal spectral width value only quantitatively indicates the most basic amount of self-similar random shapes and phenomena. As the formerly used roughness index, it is difficult to accurately determine the degree of road. Moreover, the road surface is three-dimensional, thus it is not comprehensive and irrational to resort one-dimensional array to characterize the three-dimensional characteristics.

## 5. Spectral Width Spectral Width Value, Human Body Acceleration RMS and IRI Analysis

In order to reflect the difference of the road frequency, the  $n$  in the (7) was taken 1.6, 1.8, 2.2 and 2.4 respectively, correspondingly denoted as sample NO 1,2,3,4. Simulate the road roughness sequence with the same IRI value and their IRI values are all 1.5. Similarly, we can draw that the corresponding multi-fractal spectral width value with the road sections with the same IRI value under different grades, as shown in Fig.6.

Fig. 6 shows a good linear relationship exists between the different frequencies of spectral width values and the body acceleration in the same IRI. Different frequencies will reflect on the road roughness micro-structure, while the multi-fractal spectrum well reflects the multi-fractal spectrum width value for easy distinguishing.

Table 2 Information of road with the same IRI value

section	IRI (m/km)	spectral width	RMS(m/s <sup>2</sup> )
1	1.5	0.57807	0.1645
2	1.5	0.62239	0.1882
3	1.5	0.70001	0.2477
4	1.5	0.74375	0.2802
5	4.5	0.55285	0.4685
6	4.5	0.68805	0.5378
7	4.5	1.0017	0.6408
8	4.5	0.79565	0.5789
9	7.7	0.45553	0.7021
10	7.7	0.51813	0.8226
11	7.7	0.68732	0.9585
12	7.7	0.9087	1.061
13	9.0	0.73655	0.797
14	9.0	0.88511	0.9863
15	9.0	1.0207	1.2409
16	9.0	1.0514	1.4315

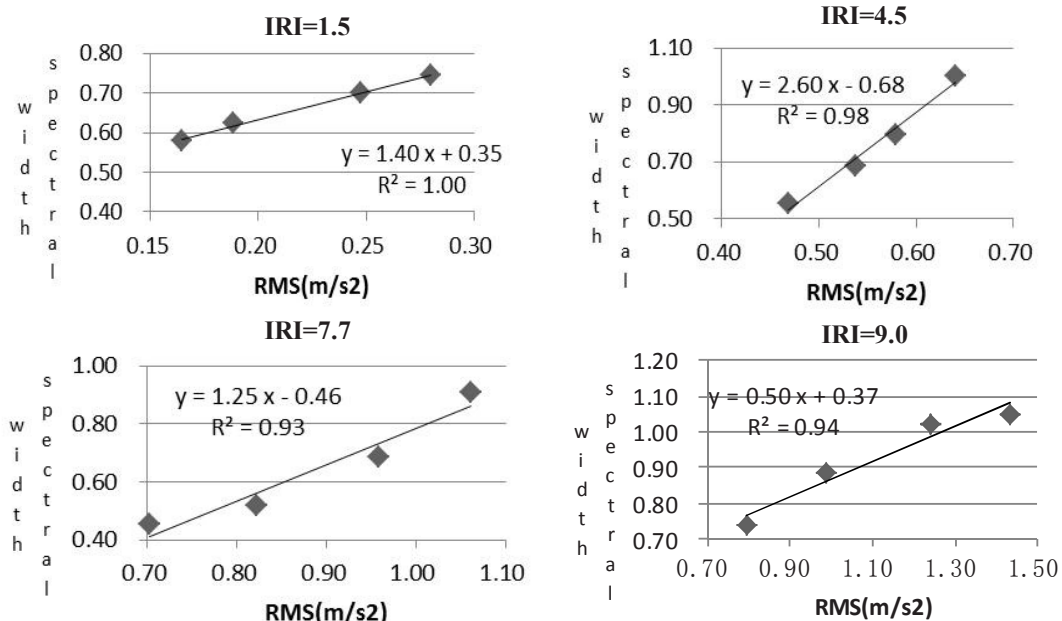


Fig. 6. Relationship between spectral width value with RMS

## 6. Human Body Bump Index

Considering the IRI is a traditional road roughness characterization parameters and to reflect the continuity between the traditional characterization parameters multi-fractal parameters, connecting IRI with multi-fractal spectrum spectral width value  $\Delta a$ , a new road roughness parameter is emerged, which is the body bump index R.



Due to the phenomenon of fat tail existing in the road roughness sequence, that is, the relationship between the rate of power function, the expression is written as the exponential form; because most of the measured pavement multi-fractal spectrum width value are less than 1, in order to make the data easier to identify, the  $\Delta a$  is changed as  $(2+\Delta a)$ , thus, the definition formula can be expressed as:

$$R = (IRI)^{(2+\Delta a)} \quad (10)$$

When the value of multi-fractal spectrum spectral width is unchanged, IRI will decrease or increase as the fluctuation degree of the road surface (absolute measure), which makes the body bump index reduce or increase. Similarly, when the IRI remains the same, the road spectrum frequency will change, that is, the multi-fractal spectrum spectral width value decreases or increases, which leads to the body bump index also increasing or decreasing and therefore make up for the defect of the IRI's insensitive to frequency. Summarily, human body bump index reflects not only the undulation of the road surface conditions from the macroscopic structure, but also the complexity of its internal structure from the microcosmic structure. In future work, real measurement proceeding of pavement samples with different pavement level will be achieved. Employ the IRI, the human acceleration RMS and human bumping index respectively to evaluate all the samples to figure out the performance of human bumping index.

## 7. Conclusion

The multi-fractal spectrum width values can not only reflect the irregularity of longitudinal profile, but also can fine depicting the characteristics of the road locally. But the results of road surface simulation in each grades based on Fourier inverse transformation show there is no unique relation between multi-fractal spectral width and road roughness in different grades. By using the Fourier inverse transformation method, simulating out the road roughness at all levels. The paper initially proposes the spectral width value and IRI-based human body bumping index as the comprehensive evaluation parameter. Compared with the traditional indicators, human body bumping index have both the pavement relative measurement (spectral width value) and the absolute measure (IRI) is able to be a preferable supplement of current indices.

## Acknowledgements

This research is supported by the China National Science Foundation Grant No. 51138003 and Grant No. 61102038, and the Natural Science Foundation of Heilongjiang Province Grant No.QC2011C097.

## References.

- LIU Wan-yu, ZHANG Lei, XIE Kai. Analysis on Measuring Technology of Road-roughness and Its Development. *Industrial Measurement*, 2007, 17(1): 9-12.
- SONG Yong-gang. Study of relationship between road surface evenness and ride quality. *Road Machinery & Construction Mechanization*. 2005, (12):18~21.
- ZHANG Yong, GUAN Wei. Complexity measure of traffic flow time series. *Journal of Traffic and Transportation Engineering*.2009.4
- Kantelhardt J.W, Zschiegner S.A, Koscielny B.E, Havlin S, Bunde A, Stanley H.E, Multi-fractal Detrended Fluctuation Analysis of Nonstationary Time Series. *Physical A*, 2002, 316(1-4):87-114.
- Li H, Ding Z J, Wu Z Q. Multi-fractal behaviour of the distribution of secondary-electron-emission sites on solid surfaces. *Phys Rev B*, 1995, 51:13554
- Lee C K, Lee S L. Multi-fractal scaling analysis of reactions over fractal surfaces. *Surface Science*, 1995, 325:294
- Wang B, Wang Y, Wu Z Q. Multi-fractal behavior of solid-on-solid growth. *Solid State Commun*, 1995, 96:69.
- Xie Weidong, Wang Lei, She Yini. Application of Random Signals to Road Roughness Simulation. *Journal of Vibration, Measurement & Diagnosis*,2005, 25(2): 126-130
- Box G.E.P. &Pierce D.A. Distribution of Residual Autocorrelations in Autoregressive-integrated Moving Average Time Series Models. *Journal of the American Statistical Association*, 1970, 65(332): 1509-1526